Supplement of Atmos. Chem. Phys., 26, 6257–6281, 2026
https://doi.org/10.5194/acp-26-6257-2026-supplement

Atmospheric Chemistry and Physics
Open Access
EGU

Supplement of

Fine and coarse dust radiative impact during an intense Saharan dust outbreak over the Iberian Peninsula – long-wave and net direct radiative effect

María Ángeles López-Cayuela et al.

Correspondence to: Carmen Córdoba-Jabonero (cordobajc@inta.es)

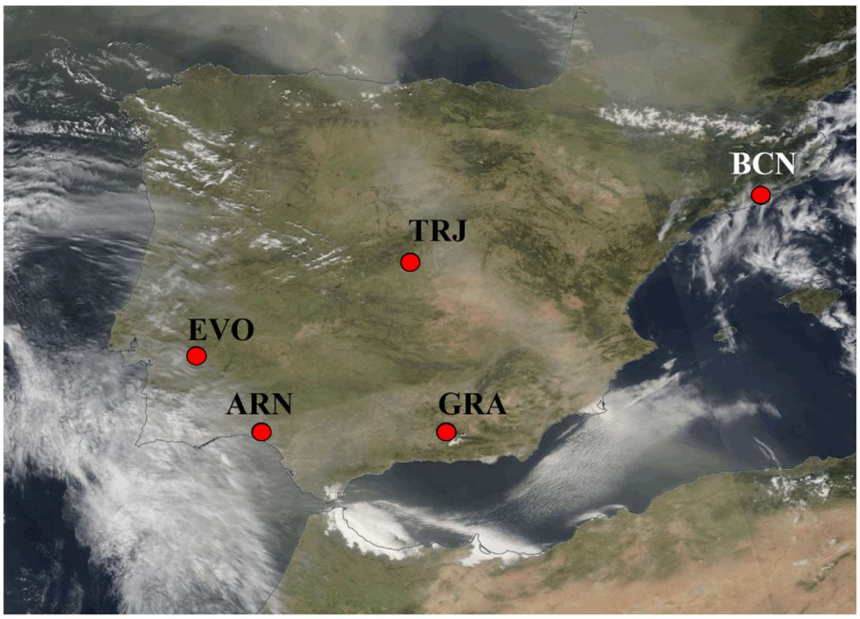

Figure S1. MODIS image of the corrected reflectance over the Iberian Peninsula on 31 March 2021. The five Iberian lidar stations are marked with a red dot (from North-East to South-West in the Iberian Peninsula): Barcelona (BCN), Torrejón/Madrid (TRJ), Évora (EVO), Granada (GRA), and El Arenosillo/Huelva (ARN) sites.

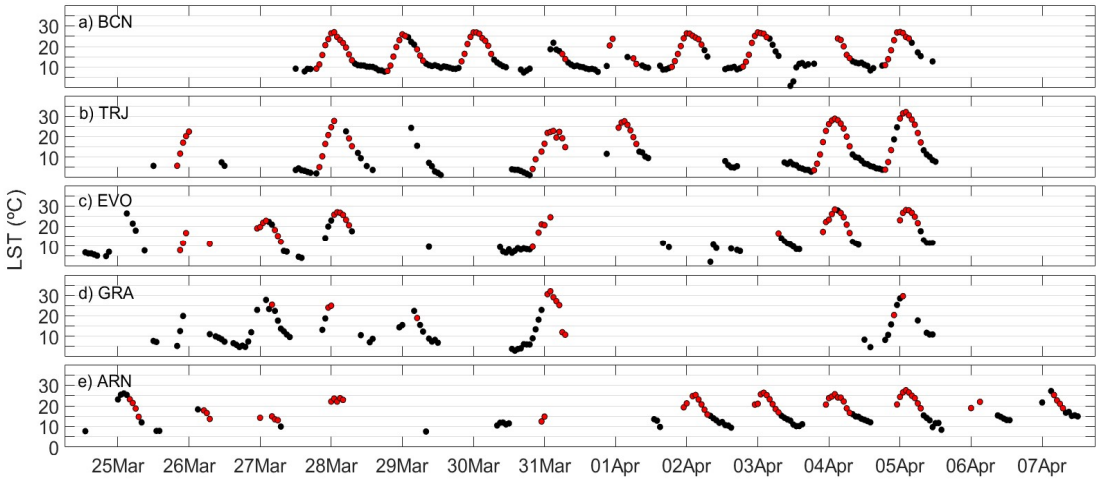

Figure S2. Hourly land surface temperature (LST) at the five Iberian lidar stations (from NE to SW, by decreasing latitude): (a) Barcelona (BCN), (b) Torrejón/Madrid (TRJ), (c) Évora (EVO), (d) Granada (GRA) and (e) El Arenosillo/Huelva (ARN). The associated uncertainty is added as a shaded area, although is so small that it is almost imperceptible. The red dots represent the values coincident with lidar measurements.

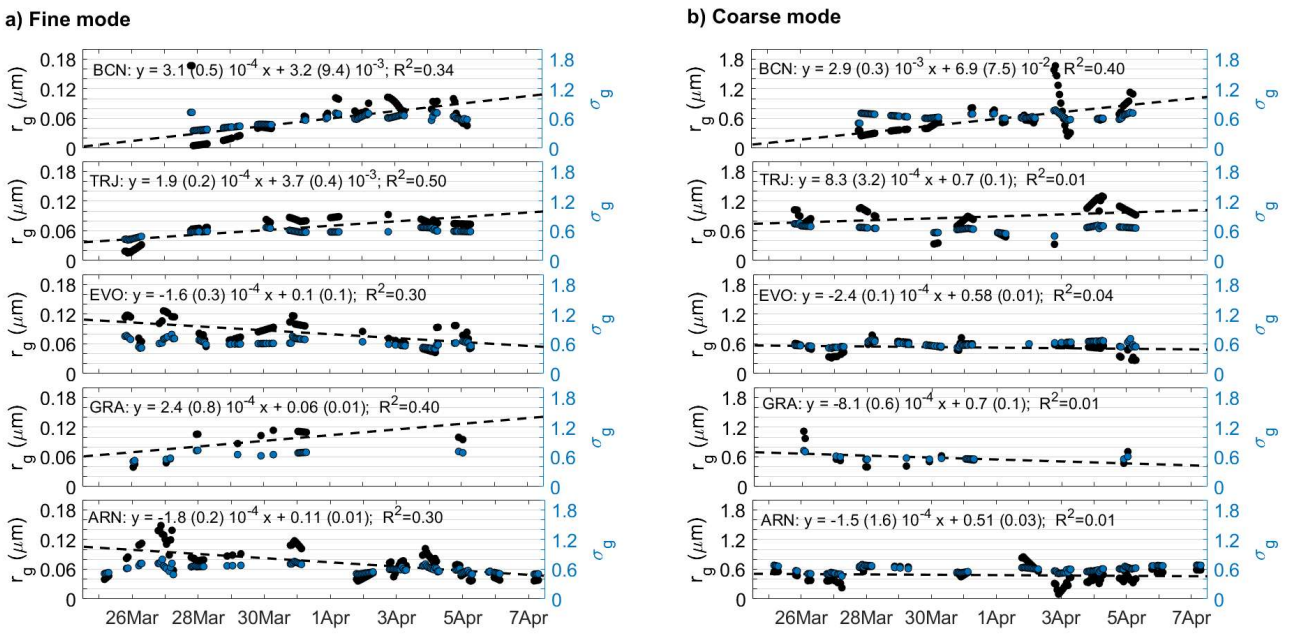

Figure S3. Hourly geometric median radius (r_g, μm; in black), and standard deviation (σ_g, μm; in blue), as derived from AERONET data (see Eq. 1), at the five lidar stations (from NE to SW, by decreasing latitude): Barcelona (BCN), Torrejón/Madrid (TRJ), Évora (EVO), Granada (GRA) and El Arenosillo/Huelva (ARN) for: a) the fine mode, and b) the coarse mode. The dashed lines represent the linear fitting along the period. The equation of the linear fitting is also shown.

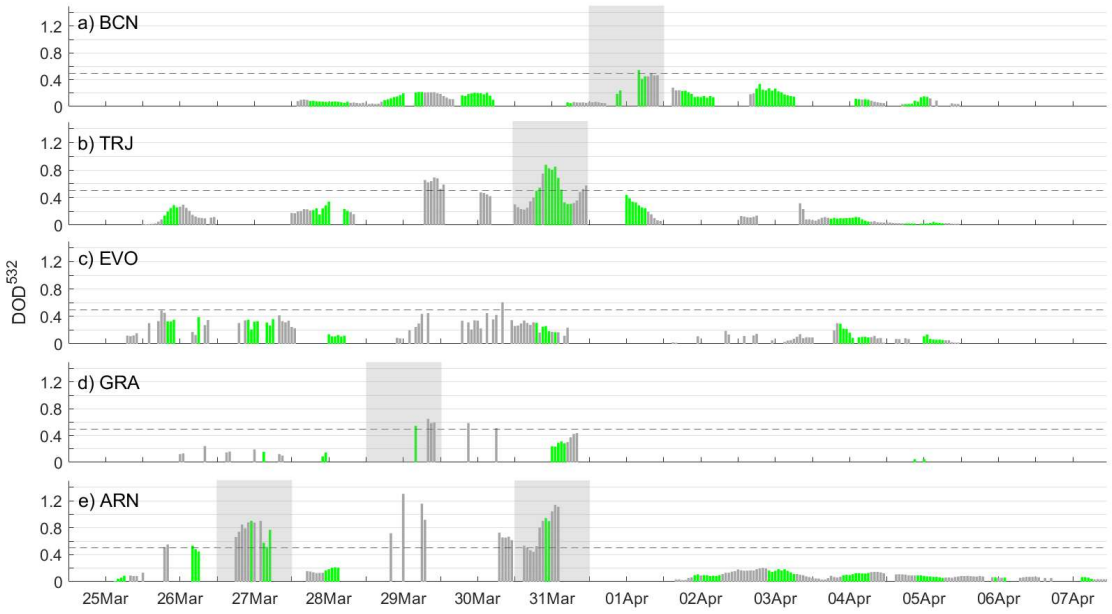

Figure S4. Temporal evolution of the total dust optical depth at 532 nm (DOD^{532}) over the five Iberian lidar stations as latitude decreases (from up to down panels): a) BCN, b) TRJ, c) EVO, d) GRA, and e) ARN. The green bars correspond to the profiles used in the LW simulations. The dashed line corresponds to DOD^{532}=0.5. Days with hourly DOD^{532} > 0.5 are marked in shadow.

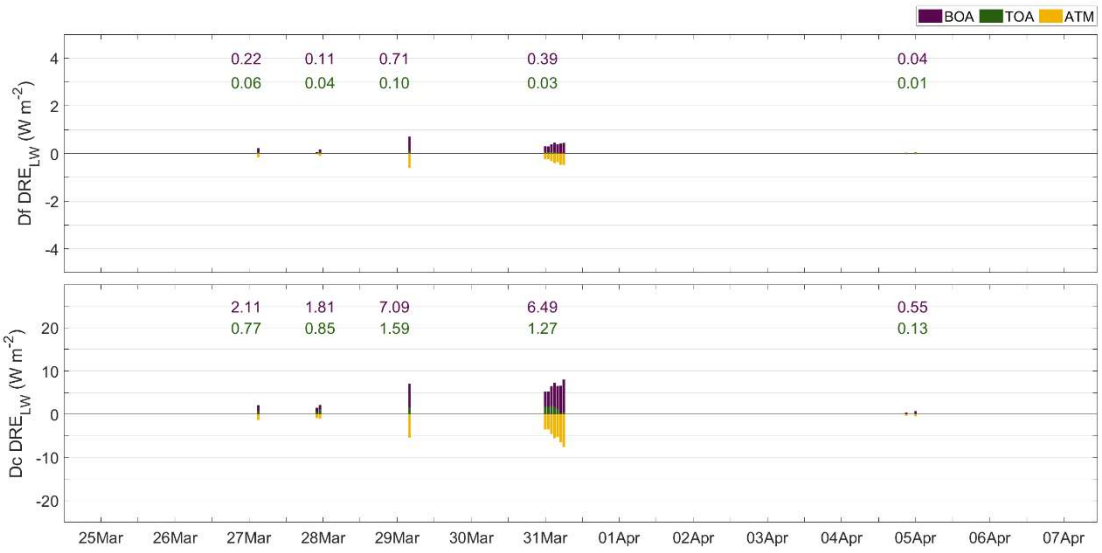

Figure S5. Dust direct radiative effect in the long-wave range (DRE_{LW}, W m^{-2}) at BOA (purple), TOA (green) and in the atmosphere (ATM, yellow) at the GRA station, as induced by the (top) fine dust (Df), and (bottom) coarse dust (Dc) particles.

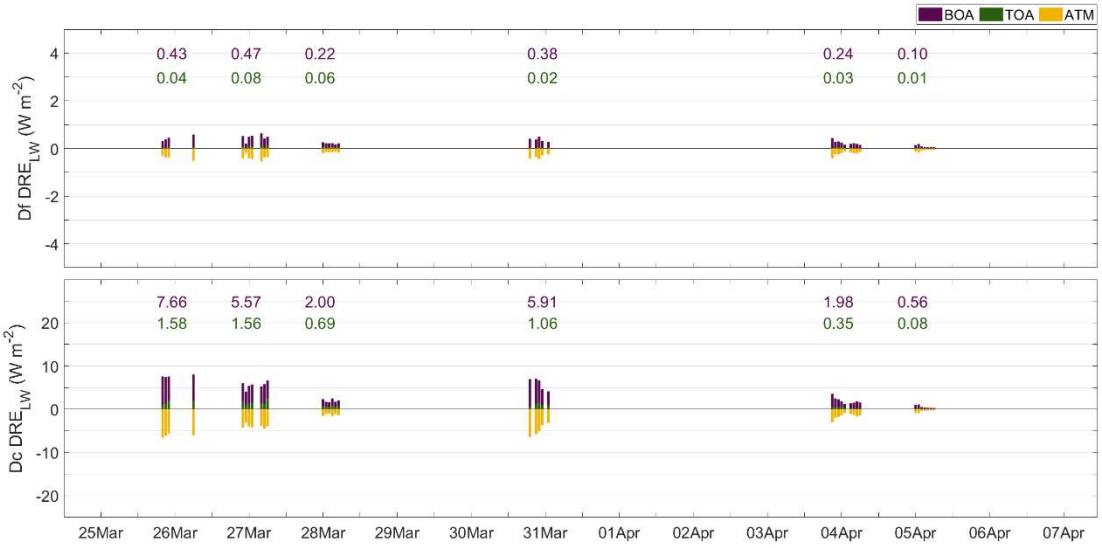

Figure S6. The same as Fig. S5, but at the EVO station.

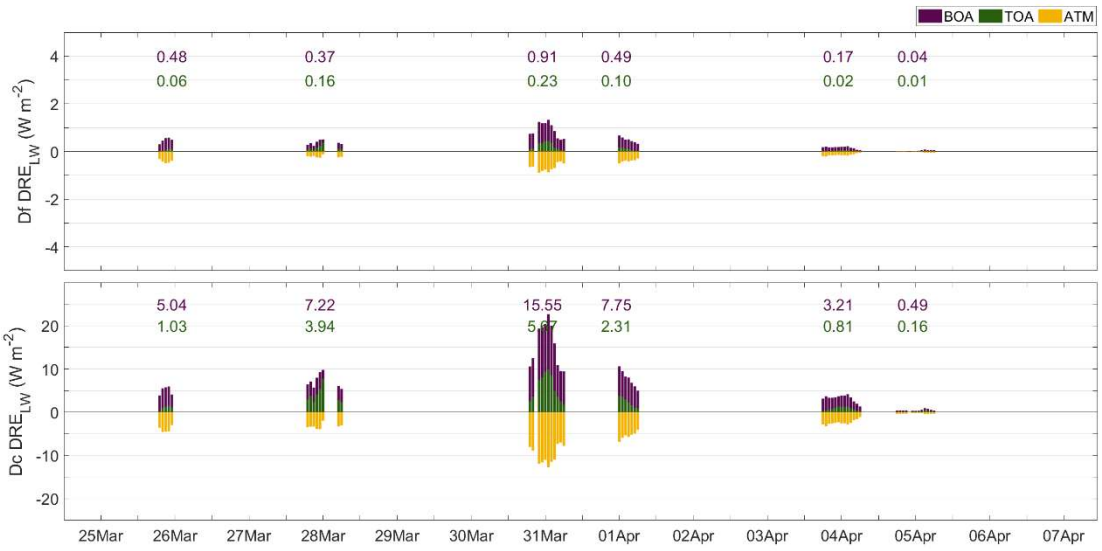

Figure S7. The same as Fig. S5, but at the TRJ station.

Figure S8. The same as Fig. S5, but at the BCN station.

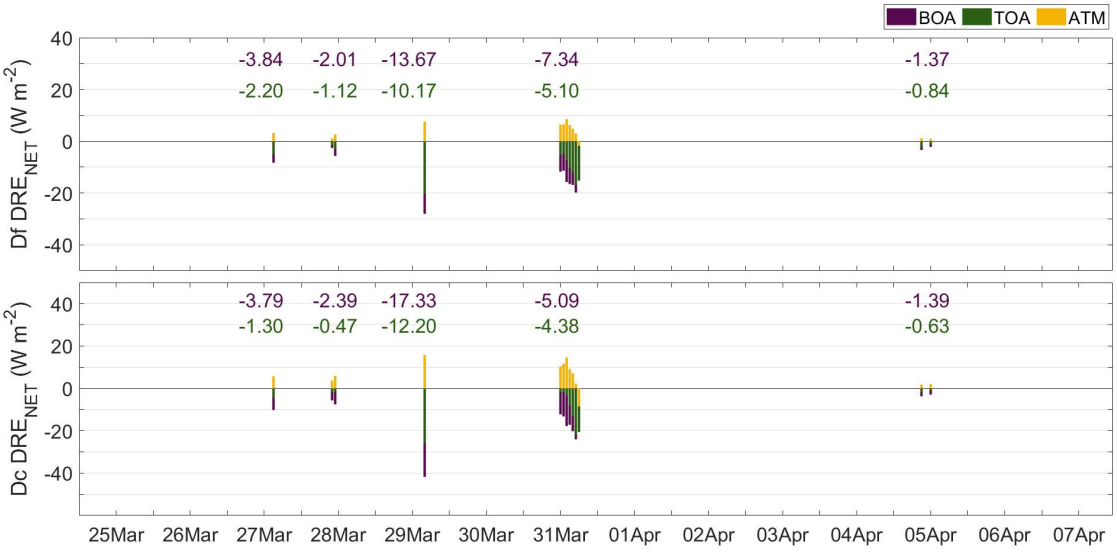

Figure S9. Dust direct radiative effect in the net range (DRE_{NET}, W m^{-2}) at BOA (purple), TOA (green) and in the atmosphere (ATM, yellow) at the GRA station, as induced by the (top) fine dust (Df), and (bottom) coarse dust (Dc) particles.

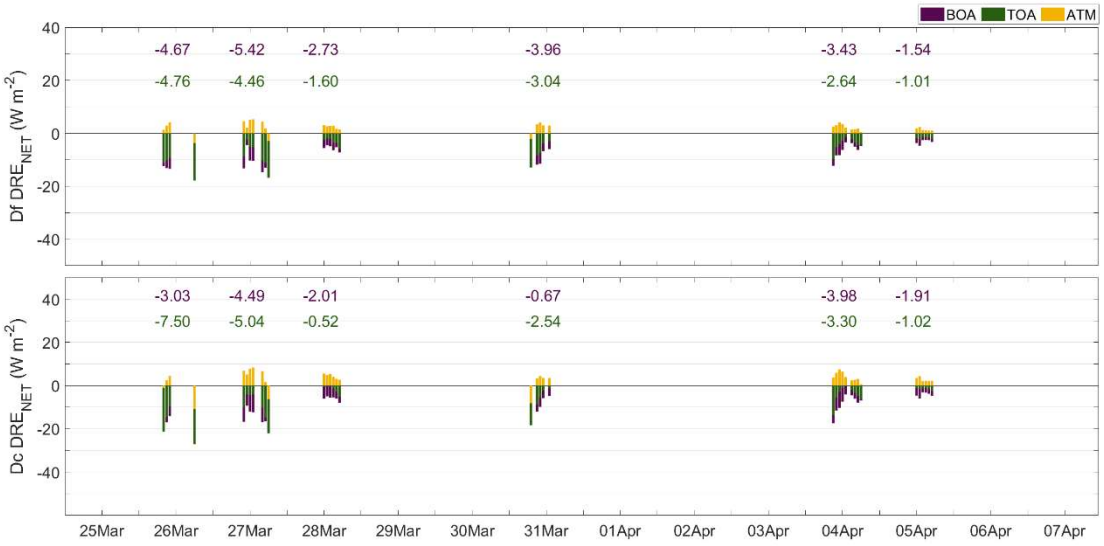

Figure S10. The same as Fig. S9, but at the EVO station.

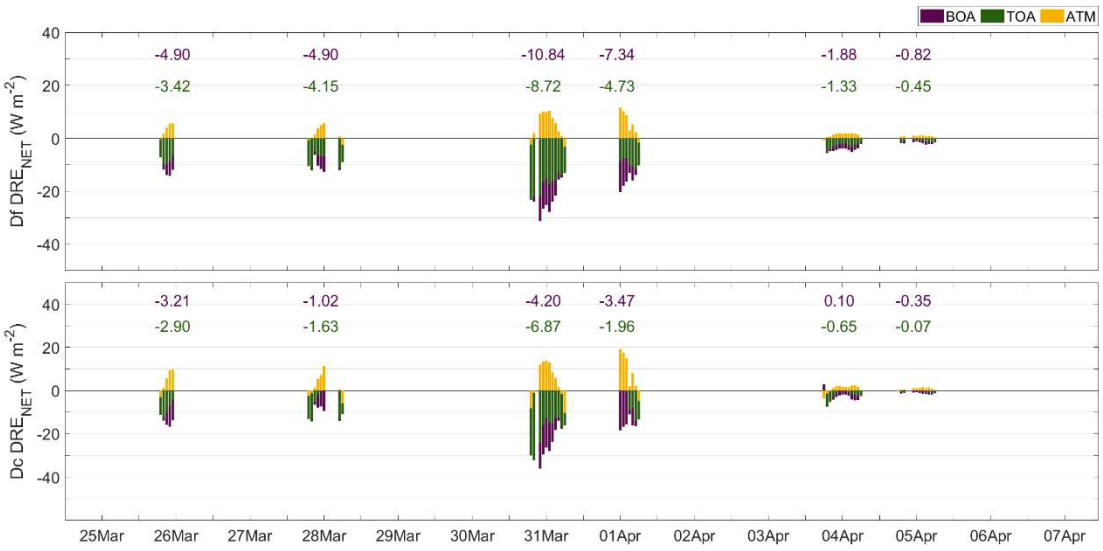

Figure S11. The same as Fig. S9, but at the TRJ station.

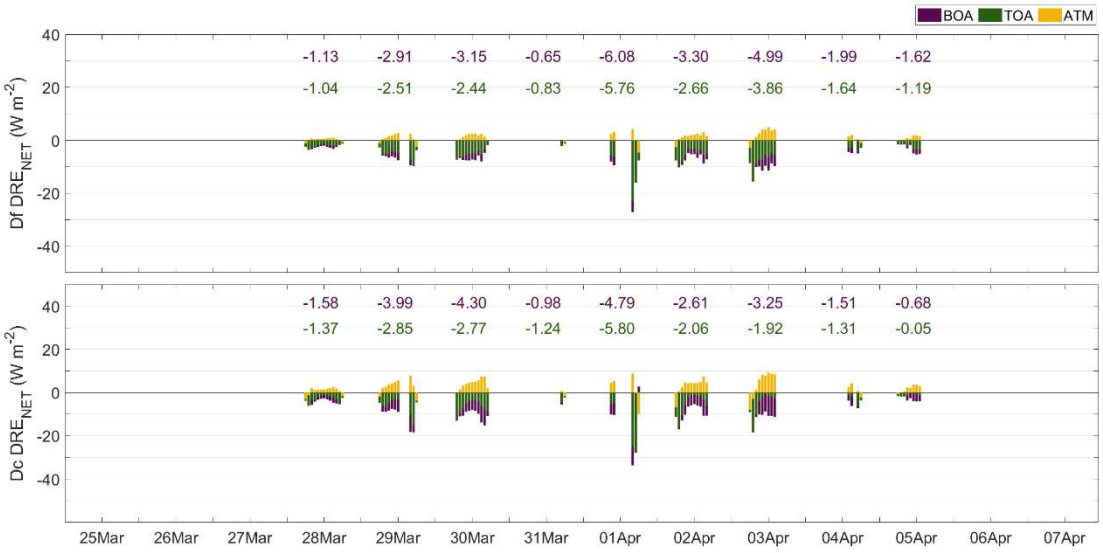

Figure S12. The same as Fig. S9, but at the BCN station.

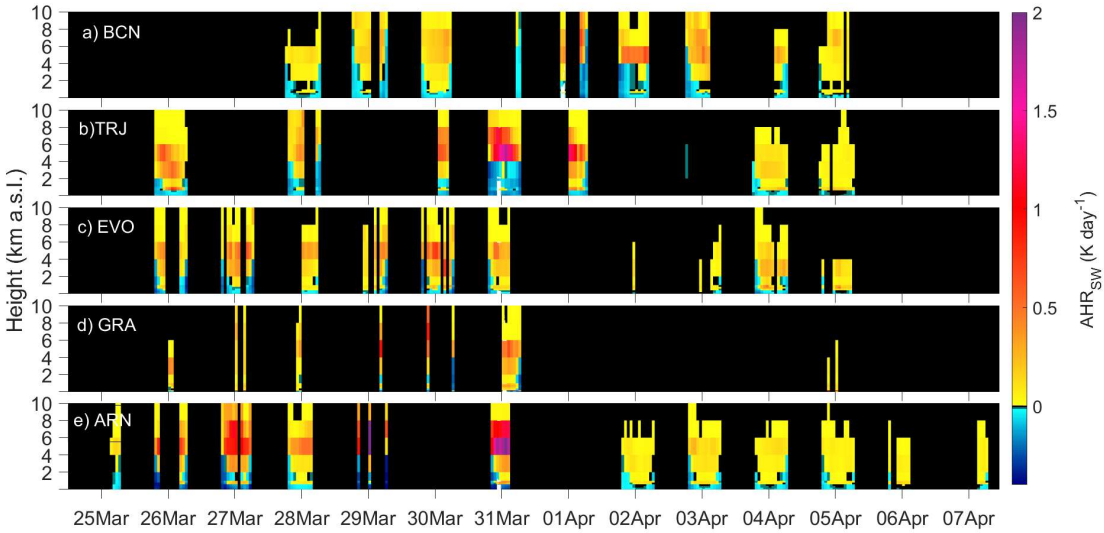

Figure S13. Vertical distribution of the aerosol heating rates in the SW range (AHR$_{SW}$, K day^{-1}) corresponding to DD particles at the five Iberian lidar stations (from North-East to South-West, by decreasing latitude): a) BCN, b) TRJ, c) EVO, d) GRA and e) ARN.

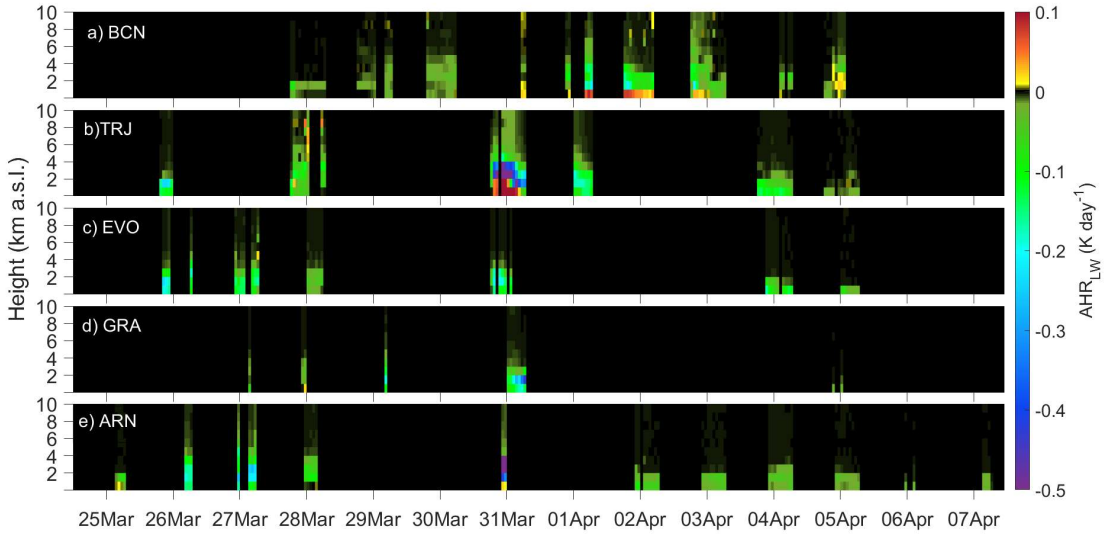

Figure S14. The same as Fig. S13, but in the LW range (AHR_{LW}, K day^{-1}).

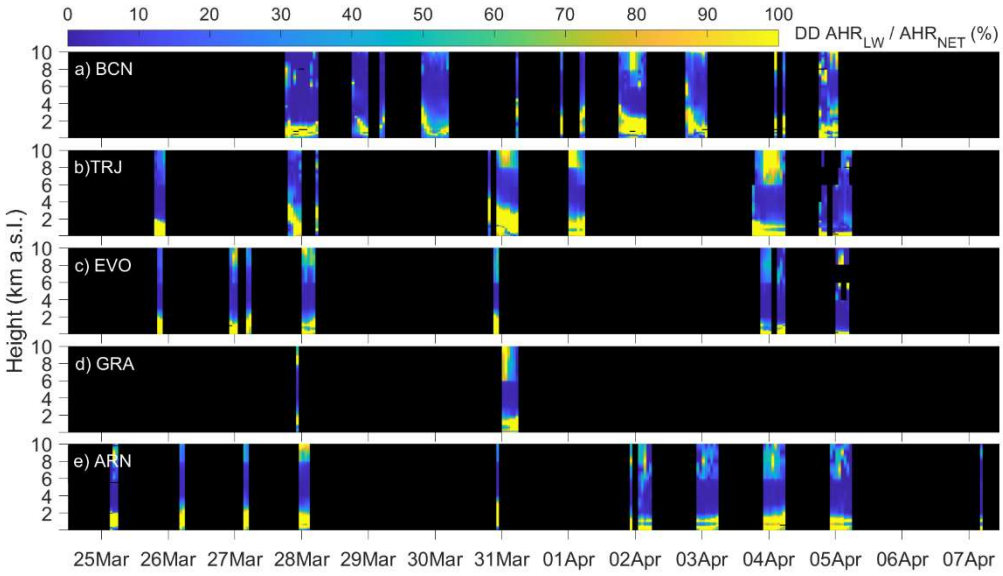

Figure S15. Vertical distribution of the LW-to-net aerosol heating rate ratio (AHR_{LW}/AHR_{NET} %) corresponding to DD particles at the five Iberian lidar stations (from North-East to South-West, by decreasing latitude): a) BCN, b) TRJ, c) EVO, d) GRA and e) ARN.

Table S1. Details of the location of the five lidar stations (and institutions) together with the period of the dust outbreak lasting over each one. The term 'a.s.l.' stands for 'above sea level'.

	El Arenosillo/Huelva (ARN), Spain	Granada (GRA), Spain	Évora (EVO), Portugal	Torrejón/Madrid (TRJ), Spain	Barcelona (BCN), Spain
Institution	Spanish Institute for Aerospace Technology (INTA)	Andalusian Institute for Earth System Research (IISTA-CEAMA), and University of Granada (UGR)	University of Évora (UE)	Spanish Institute for Aerospace Technology (INTA)	Polytechnic University of Catalonia (UPC)
Location	37.11° N 6.73° W 40 m a.s.l.	37.16° N 3.61° W 680 m a.s.l.	38.57° N 7.91° W 293 m a.s.l.	40.49° N 3.46° W 568 m a.s.l.	41.39° N 2.11° E 115 m a.s.l.
Period	25 March – 7 April	25 March – 5 April	25 March- 5 April	26 March – 5 April	28 March – 5 April
Instrument	Polarized Micro-pulse lidar	Raman lidar	Raman lidar	Polarized Micro-Pulse lidar	Polarized Micro-Pulse lidar